



Molecular cloning and functional characterization of borneol dehydrogenase from the glandular trichomes of *Lavandula x intermedia*

Lukman S. Sarker, Mariana Galata, Zerihun A. Demissie, Soheil S. Mahmoud*

University of British Columbia, Okanagan Campus, Department of Biology, 3333 University Way, Kelowna, BC, Canada V1V 1V7

ARTICLE INFO

Article history:

Received 14 August 2012
and in revised form 28 September 2012
Available online 8 October 2012

Keywords:

Lavandula x intermedia
Essential oil
Camphor
Alcohol dehydrogenases
Monoterpene synthases

ABSTRACT

Several varieties of *Lavandula x intermedia* (lavandins) are cultivated for their essential oils (EOs) for use in cosmetic, hygiene and personal care products. These EOs are mainly constituted of monoterpenes including camphor, which contributes an off odor reducing the olfactory appeal of the oil. We have recently constructed a cDNA library from the glandular trichomes (the sites of EO synthesis) of *L. x intermedia* plants. Here, we describe the cloning of a borneol dehydrogenase cDNA (*LiBDH*) from this library. The 780 bp open reading frame of the cDNA encoded a 259 amino acid short chain alcohol dehydrogenase with a predicted molecular mass of ca. 27.5 kDa. The recombinant LiBDH was expressed in *Escherichia coli*, purified by Ni-NTA agarose affinity chromatography, and functionally characterized *in vitro*. The bacterially produced enzyme specifically converted borneol to camphor as the only product with K_m and k_{cat} values of 53 μM and $4.0 \times 10^{-4} \text{ s}^{-1}$, respectively. The *LiBDH* transcripts were specifically expressed in glandular trichomes of mature flowers indicating that like other *Lavandula* monoterpene synthases the expression of this gene is regulated in a tissue-specific manner. The cloning of *LiBDH* has far reaching implications in improving the quality of *Lavandula* EOs through metabolic engineering.

© 2012 Elsevier Inc. All rights reserved.

Introduction

Lavenders are small aromatic shrubs cultivated worldwide for their essential oils (EOs)¹ – a blend of mono- and sesquiterpenoid alcohols, esters, oxides, and ketones – which are extensively used in cosmetics, hygiene products and alternative medicines. Around 50–60 monoterpenes have been identified in different lavender varieties, although only a few predominate the characteristic EO of a given species [1]. The most abundant monoterpenes found in lavenders include linalool, linalool acetate, borneol, camphor, and 1,8-cineole. Among these, camphor, linalool, and linalool acetate are key determinants of the lavender EO quality [1,2]. EOs with a high linalool and linalool acetate to camphor ratio are considered to be of “high quality”, and thus are used in cosmetic products and aromatherapy [3,4]. EOs added to alternative medicines are typically rich in camphor and 1,8-cineole. In particular, oils containing high camphor content are used in inhalants to relieve coughs and colds [5], and as active ingredients in liniments and balms used as topical analgesics [6]. Camphor has also been

considered as a potential radio sensitizing agent, and has been used in oxygenating tumors prior to radiotherapy [7,8]. The exact physiological role of camphor *in planta* is not clear, although substantial evidence indicates that this metabolite mediates plant–plant interactions and has a role in allelopathy [9,10].

Lavandula EOs destined for perfumery are typically obtained from *Lavandula angustifolia* species, and contain high levels of linalool and linalool acetate and negligible quantities of the other monoterpenes. Oils marketed to the alternative medicine sector are typically obtained from *Lavandula latifolia* plants, which accumulate high levels of linalool, camphor and 1,8-cineole, but no linalool acetate. The EOs obtained from *L. x intermedia* plants, which result from natural crosses between *L. latifolia* and *L. angustifolia* species, contain a mixture of monoterpenes present in both parental lines, and are mainly utilized in personal care and hygiene products including soaps, shampoos, mouth washes, and industrial and household cleaners, among others [11].

In lavenders, the biosynthesis of camphor, along with other EO constituents, takes place in glandular trichomes or oil glands, through a series of relatively simple biochemical reactions (Fig. 1). The biosynthetic pathway for camphor was previously defined based on precursor feeding experiments [12]. Like other monoterpenes, camphor is derived from isopentenyl diphosphate (IPP) and dimethylallyl diphosphate (DMAPP), the universal precursors to all isoprenoids. The head-to-tail condensation of IPP and DMAPP initially generates geranyl diphosphate (GPP), the linear

* Corresponding author.

E-mail address: soheil.mahmoud@ubc.ca (S.S. Mahmoud).

¹ Abbreviations used: EO(s), essential oil(s); TPS(s), terpene synthase(s); mTPS(s), monoterpene synthase(s); sTPS(s), sesquiterpene synthase(s); GPP, geranyl diphosphate; NPP, neryl diphosphate; LiLINS, *L. x intermedia* linalool synthase; LiBDH, *L. x intermedia* borneol dehydrogenase; SDR, short chain dehydrogenase/reductase.

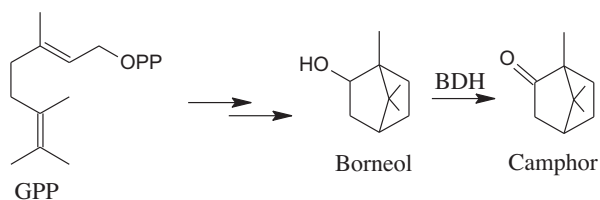


Fig. 1. Proposed pathway for camphor biosynthesis. Multiple arrows indicate involvement of multiple enzymes. GPP, geranyl diphosphate; OPP, diphosphate moiety; BDH, borneol dehydrogenase.

C₁₀ precursor to all regular monoterpenes, which is subsequently cyclized and hydrolyzed to borneol through the catalytic activities of bornyl diphosphate synthases and borneol synthases, respectively [13,14]. Oxidation of borneol will then generate camphor through the catalytic activity of borneol dehydrogenase (BDH) [10,15]. So far a specific plant BDH has not been reported. However, a non-specific (accepting multiple substrates) short chain alcohol dehydrogenase (SDR) from *Artemisia annua* was recently shown to produce the corresponding ketones from a number of monoterpene alcohols, including borneol, as a minor substrate [16].

Members of the SDR super-family of enzymes, which are found in all living organisms, generally share low sequence similarity level and have affinity towards structurally diverse substrates. The C-terminal domains of SDRs determine substrate specificity and can be highly variable between different SDR members [17,18]. The only common characteristic feature of all SDRs are their short size (about 250 amino acids), the co-factor binding Rossmann-fold scaffold, and their ability to bind NAD(P)(H). The Rossmann-fold scaffold is characterized by a twisted parallel β -sheet flanked on either side by 3–4 α -helices [19]. SDRs are classified into five sub-families denoted as “classical”, “extended”, “intermediate”, “complex”, and “divergent” according to sequence combinations in their conserved motifs residing in the cofactor binding and active sites [17,20]. The conserved motifs that define the classical SDRs sub-family members are TGxxx[AG]xG and YxxxK. The Gly rich motif in the cofactor-binding site determines the protein’s cofactor (NAD⁺ or NADP⁺) specificity, while adjacent serine and lysine residues flank the tyrosine based catalytic center [17]. Tyr is a catalytic residue, and Lys has a dual function as it interacts with the coenzyme and lowers the pK_a value of the Tyr through a strong electrostatic influence [21].

SDR enzymes play important roles in the metabolism of lipids, proteins, and carbohydrates. They have also demonstrated roles in specialized metabolism in plants [10,17]. Recently, a few SDRs have been reported from *A. annua* and *Zingiber zerumbet*, where they are responsible for the biosynthesis of mono- and sesquiterpenoid ketones from multiple substrates [10,16]. In this study, we employed a homology-based cloning strategy to clone a SDR from *L. x intermedia* oil gland library (LiBDH), which converts borneol into camphor *in vitro*.

Material and methods

EST database analysis and BDH candidate selection

We have recently reported the construction of a cDNA library and the corresponding EST database for the floral glandular trichomes of mature (30% in bloom) *L. x intermedia* flowers [22]. Based on homology to known SDRs, four full-length BDH candidates were selected and fully sequenced prior to further analysis.

Recombinant protein expression and enzyme assay

The predicted ORFs for BDH candidates were amplified by PCR using iProof high fidelity DNA polymerase (Bio-Rad, USA) and

specific primer sets containing appropriate restriction enzyme sites (Table 1) for cloning in an expression vector. The Amplicons were digested with Nde I and EcoR I/Xho I restriction enzymes and ligated into pET41b(+) bacterial expression vector where it was fused to sequences encoding eight C-terminus Histidine residues to facilitate purification by Ni-NTA agarose affinity chromatography (EMD Chemicals, Darmstadt, Germany). To produce the recombinant protein, *Escherichia coli* Rosetta™ (DE3)plysS cells (EMD Chemicals, Darmstadt, Germany) were transformed with individual constructs, grown to log phase at 20 °C in Luria–Bertani (LB) media supplemented with 30 mg/L Kanamycin and 34 mg/L chloramphenicol, and induced with isopropyl- β -D-thiogalactopyranoside (IPTG) at a final concentration of 0.5 mM. The induced cells were chilled on ice for 15–20 min, collected by centrifugation at 3,220g and 4 °C for 20 min, and stored at –80 °C overnight. The stored cells were resuspended in Novagen bind buffer (0.3 M NaCl, 50 mM Na₂HPO₄, 10 mM imidazole, pH 8.0; EMD Chemicals, Germany) containing 1 mM protease inhibitor phenylmethanesulfonyl fluoride (PMSF), and sonicated on ice using a Sonic Dismembrator Model 100 (Fisher Scientific, Ottawa, ON, Canada) to complete bacterial membrane disruption. The cell debris were removed by centrifugation at 15,000g and 4 °C for 15 min (Sorvall, USA), and the recombinant proteins harvested from the soluble fraction by Ni-NTA agarose affinity chromatography (EMD Chemicals, Germany) following the manufacturer’s procedure. Protein samples were resolved by sodium dodecyl sulfate polyacrylamide gel electrophoresis (SDS–PAGE) and visualized by staining with Coomassie Brilliant Blue. Protein concentration was determined by Bradford Assay (Bio-Rad).

Initially, enzyme assays were performed in 5 ml of 100 mM sodium phosphate buffer [12,23,24] (pH 8.0), containing 40 μ g of the enzyme, 1 mM NAD⁺, and 0.5 mM substrate (borneol). After overnight incubation at 30 °C with 150 r.p.m shaking, assay products were extracted into 1 ml pentane and concentrated ~50 times before analysis by GC–MS (see below). For linear kinetics study, assays were performed in 2 ml reaction volume (keeping reagent concentrations as before) at five different time points: 1, 2, 4, 8, and 16 h. The optimum temperature was determined from a set of reactions performed at 27, 30, 32, 35 and 37 °C. The optimum pH was determined by performing assays at pH 7.0, 7.5, 8.0, 8.5, 9.0 and 10.0 using MOPS for pH 7.0 and pH 7.5, sodium phosphate for pH 8.0, TAPS for pH 8.5, and CAPSO for pH 9.0 and 10.0 as a buffer, respectively. All assays were performed in duplicate or triplicate.

To construct the Michaelis–Menten saturation curve, enzyme assays ($n = 5$) were performed at optimum temperature (32 °C) and pH (8.0) for 30 min in 1 ml reaction volume containing 100 mM sodium phosphate buffer, 1 μ M enzyme, 1 mM NAD⁺, and substrate concentration of 5, 25, 50, 100, 200, 400 μ M and 1 mM. Assay progress was monitored by measuring the conversion of NAD⁺ to NADH at 340 nm using a Lambda 25 UV–visible spectrometer (Perkin-Elmer). The kinetic parameters of the enzyme were determined from a Michaelis–Menten saturation curve constructed using SigmaPlot software version v.10.00 (Systat Software, Germany).

Table 1
Oligonucleotides used in this study.

| Primer type | Target gene | Primers |
|-------------|----------------|--------------------------------------|
| Full length | LiBDH | F-5'-CCCTCATATGGCTTCAACTGTTTGGAGA-3' |
| | | R-5'-AGTCTCGAGCGAATCCATCAAATCAAAC-3' |
| qPCR | LiBDH | F-5'-AATCGGAGCGGAGCATAATCT-3' |
| | | R-5'-TAATACGGCGAGCCGAGTTCA-3' |
| | LiLINS | F-5'-ACACGCACGACAATTTGCCA-3' |
| | | R-5'-AGCCCTCCAATGAAGTGGGAT-3' |
| | β -actin | F-5'-TGTGGATTGCCAAGGCAGAGT-3' |
| | | R-5'-AATGAGCAGGCAGCAACAGCA-3' |

GC–MS analysis for the assay reaction

Assay products were analyzed using a Varian 3800 Gas Chromatographer coupled to a Saturn 2200 Ion Trap mass detector. The instrument was equipped with a 30 m × 0.25 mm capillary column coated with a 0.25 μm film of acid-modified polyethylene glycol (ECTM 1000, Altech, Deerfield, IL, USA), and a CO₂ cooled 1079 Programmable Temperature Vaporizing (PTV) injector (Varian Inc., USA). Samples were injected on-column at 40 °C. The oven temperature was initially maintained at 40 °C for 3 min, raised to 130 °C at a rate of 10 °C per minute, then to 230 °C at a rate of 50 °C per min, and finally held at 230 °C for 8 min. The carrier gas (helium) flow rate was set to 1 ml per min. The identities of products were confirmed by comparing their retention times and mass spectra to those of authentic standards (from our collection) analyzed under the same conditions. EOs of *L. angustifolia*, *L. x intermedia* and *L. latifolia* flowers were distilled and analyzed as previously reported [25], and EO constituents were identified by comparison of obtained mass spectra to those of authentic standards, or to those in the NIST library. The reaction assays contained 1,8-cineole (1 mg/ml) as an internal standard.

Relative expression assay of LiBDH

Total RNA was extracted from different lavender tissues by using a plant RNA extraction kit and treated with DNase I enzyme to remove genomic DNA using Omega Bio-Tek kit, USA. Treated total RNA was reverse transcribed with Oligo (dT) (80 μM) and random hexamers (40 μM) (Custom oligos, IDT Canada) by using *M-MuLV* Reverse Transcriptase enzyme (New England Biolabs, MA, USA) following the manufacturer protocol. The transcriptional activity of *LiBDH* in 30% flowering stage and in young leaf tissues were analyzed from *L. angustifolia*, *L. x intermedia*, and *L. latifolia* by standard PCR based on the intensity of *LiBDH* bands amplified with set I cloning primers (Table 1) and *Taq* DNA Polymerase (New England Biolabs, USA). The following PCR program was used: initial denaturation at 95 °C for 5 min, followed by 95 °C for 1 min, 55 °C for 30 s and 72 °C for 1 min for 30 cycles with a final elongation at 72 °C for 5 min. The above PCR reaction was repeated for the *LiBDH* analysis from Bud-I, Anthesis, 30% flowering stage, and glandular trichome from 30% flowering stages of *L. x intermedia*. The relative abundance of *LiBDH* across *L. x intermedia* flower developmental stages and glandular trichomes was analyzed from the above lavender tissues by using CFX96™ Real Time detection system (Bio-Rad, USA). cDNA for relative transcript analysis was synthesized using iScript cDNA synthesis kit from Bio-Rad according to manufacturer's instructions. SsoFast™ Eva- Green® Supermix (Bio-Rad, USA) along with approximately 150 ng of cDNA as a template and 500 nM of each of the primers in 20 μl reaction volume. Gene specific primers (Table 1) used in quantitative real-time PCR experiments were designed using the IDT primer quest software (<http://www.idtdna.com/Scitools/Applications/Primerquest/>) targeting 120–200 base-pairs (bp) fragment size. The following program was used for real time PCR: 95 °C for 30 s followed by 40 cycles of 5 s at 95 °C and 30 s at 58 °C. Normalized expression values ($\Delta\Delta C_T$) of *LiBDH* and *LaLINS* were calculated by CFX96™ data manager (Bio-Rad, USA) using β -actin as a reference gene.

Phylogenetic analysis

The phylogenetic tree was constructed using the default parameters of PhyML software available at <http://www.phylogeny.fr> [26]. PhyML employs MUSCLE software to generate multiple alignments and the maximum likelihood computational method to construct the phylogenetic tree. Classical SDRs from different plant were employed in the phylogenetic tree construction.

Results

EST database and candidate selection

A homology-based analysis of our sequences against those in TAIR and UniProt protein databases identified a total of ten ESTs as putative SDRs. Among these, two ESTs corresponded to singletons, while the remaining eight formed three contigs. Two contigs (Contig 1 and 2) included two EST members each, and one contig (Contig 3) contained four members. Only Contigs 1 and 3 produced ESTs that encoded full length SDRs, and thus were selected for further analysis. The full length EST corresponding to Contig 1 (designated LiSDR-1) was 1020 base pairs, with an ORF of 759 nucleotides that encoded a protein of 253 amino acids with a predicted molecular weight of 27 kDa. The other full length EST, Contig 3, (designated LiSDR-2) was 841 nucleotides long, had an ORF of 780 nucleotides that encoded a 259 amino acid protein with a predicted molecular weight of 27.5 kDa. Both proteins bore predicted mitochondrial targeting sequences, as identified by the IPSORT (<http://ipsort.hgc.jp/>), TargetP (<http://www.cbs.dtu.dk/services/TargetP/>) and PREDOTAR (<http://urgi.versailles.inra.fr/predotar/predotar.html>) online protein analysis tools. It is worth noting that all three protein analysis tools identified a mitochondrial targeting sequence for LiSDR-2. However, a mitochondrial targeting sequence for LiSDR-1 was only identified by IPSORT.

Functional analysis of recombinant LiBDH

The LiSDR-1 and LiSDR-2 proteins were expressed in *E. coli* (Rosetta (DE3)pLysS cells, and purified by Ni–NTA affinity column chromatography. Following purification, the recombinant enzymes were assayed for dehydrogenase activity with borneol as a substrate, and either NAD⁺ or NADP⁺ as a cofactor. Analysis of the assay products by GC–MS revealed that LiSDR-1 did not produce a detectable product, while LiSDR-2 (subsequently renamed LiBDH) produced camphor from borneol with 1 mM NAD⁺ (but not NADP⁺) as a cofactor (Fig. 2b). Further, assays of the recombinant LiBDH at lower NAD⁺ concentrations (0.10, 0.25, and 0.50 mM) resulted in formation of lower amounts of the product. The negative control assays, which contained all the reagents including recombinant protein extracts obtained from bacterial cells harboring the empty vector, did not produce detectable products (Fig. 2d). Also, the reverse reduction assay in which camphor was used as a substrate and NADH as a cofactor, did not produce detectable amounts of borneol or other products (data not shown). Furthermore, a recombinant *L. angustifolia* SDR and a medium chain alcohol dehydrogenase (MDR) from *L. x intermedia* (expressed and purified using the same procedures) were not able to produce detectable quantities of camphor from borneol when assayed under identical conditions. The SDR cDNA cloned from *L. angustifolia* 30% flower was obtained from our previously reported *L. angustifolia* floral cDNA library [4].

To examine the substrate specificity of the enzyme, LiBDH was also assayed with eight other monoterpenes (alpha terpineol, 1,8-cineole, citronellol, linalool, lavandulol, nerol, geraniol, and perillyl alcohol), and one sesquiterpene (farnesol) found in lavenders, and with menthol which is a common monoterpene in other *Lamiaceae* plants. Significant amount of products were not found after 12 h of incubation in any of the assays, except for those containing α -terpineol as a substrate which produced trace amounts of camphor and isoborneol. However, comparable quantities of both products were also found in negative control assays that contained α -terpineol as a substrate, indicating that these monoterpenes were produced either non-specifically, or through the action of a contaminating bacterial protein.

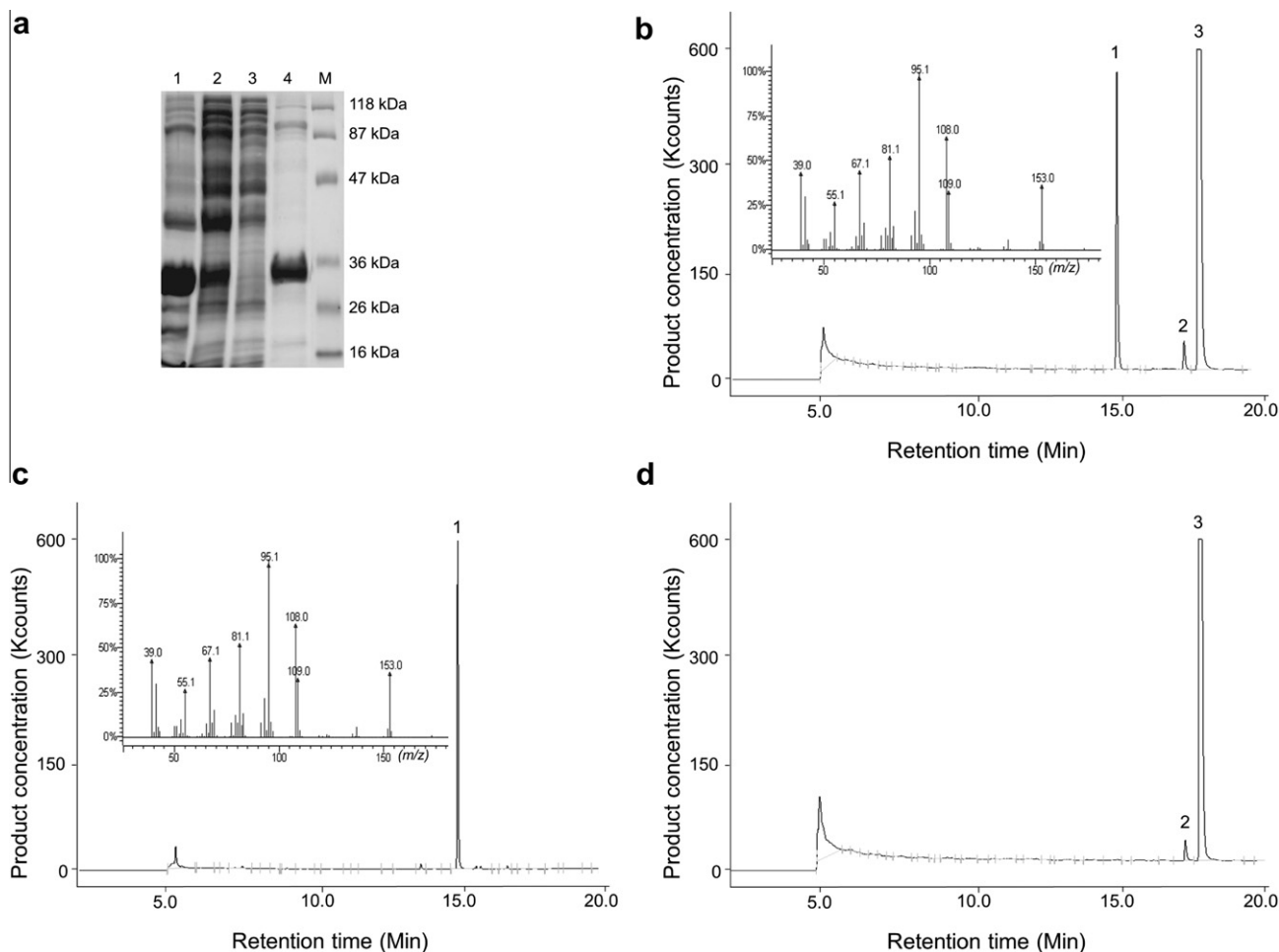


Fig. 2. Protein purification and GC–MS analysis of LiBDH. (a) SDS–PAGE stained with Coomassie blue. M: marker, 1 – pellet from induced cells, 2 – soluble fraction, 3 – flow through, 4 – LiBDH recombinant protein purified by Ni–NTA resin column. (b) GC chromatogram of LiBDH assay with mass spectrum of camphor. (c) GC chromatogram and mass spectrum of authentic camphor. (d) GC analysis of extract from the negative control. Peak-1 Camphor, peak-2 Iso borneol, peak-3 borneol.

Kinetic parameters

The recombinant LiBDH showed linear catalytic activity from 60 min to several hours (Fig. 3a). Note that the best fit line for the plotted data (Fig. 3a) did not extrapolate to the plot origin, indicating that the quantities of the product in shorter assays (less than 2 h long) were likely underestimated due to detection limitations. The optimum pH and temperature for the recombinant LiBDH were determined to be 8.0 (Fig. 3b) and 32 °C (Fig. 3c), respectively. The Michaelis–Menten enzyme saturation curve was generated using the hyperbolic enzyme kinetics analysis module of the SigmaPlot software v.10.00 (Systat Software, Erkrath, Germany) (Fig. 3d). The K_m of LiBDH was found to be $53.6 \pm 14.9 \mu\text{M}$, while its V_{max} , k_{cat} and k_{cat}/K_m were calculated to be $3.97 \times 10^{-1} \text{ pmol s}^{-1}$, $4.0 \times 10^{-4} \text{ s}^{-1}$ and $7.5 \times 10^{-6} \mu\text{M}^{-1} \text{ s}^{-1}$, respectively.

Tissue specific regulations of LiBDH

Initially a standard PCR strategy was used to study the expression pattern of LiBDH transcript in various *L. x intermedia* tissues, including leaf, bud, anthesis, and mature (30% in bloom) flowers. The results indicated that the transcripts for this gene were mostly abundant in floral glandular trichomes (Fig. 4a). Next, we employed a quantitative PCR (qPCR) approach to quantitate the expression of LiBDH mRNA in various tissues of *L. x intermedia*, including leaf, anthesis, floral tissues collected at 30% flowering

stage and secretory cells isolated from floral tissues at 30% flowering stages. The results of this experiment confirmed that the LiBDH transcripts were much more abundant (ca. 200 fold higher) in the secretory cells of glandular trichomes compared to whole flower tissue (Fig. 4b). Finally, the transcriptional activity of LiBDH in young leaves and floral tissues (30% flowering) of *L. angustifolia*, *L. x intermedia* and *L. latifolia* plants was determined by qPCR. In this experiment, the abundances of the *L. x intermedia* linalool synthase (LiLINS) transcripts were also measured as a control [4]. As expected, LiLINS mRNA was strongly expressed in flowers compared to leaves (Fig. 4c). The LiBDH transcripts were detected in both *L. angustifolia* and *L. x intermedia* flowers; however, they were much less abundant than those of LiLINS. Further, LiBDH mRNA was much less abundant in *L. latifolia* flowers compared to those of *L. angustifolia* and *L. x intermedia* plants (Fig. 4c). The relatively low expression of LiBDH mRNA paralleled the concentrations of borneol and camphor (also relatively low compared to linalool), which amounted to 0.6–2.0 mg per gram of fresh tissue for both monoterpenes, in these tissues (Fig. 4d).

Phylogenetic analysis

LiBDH exhibited a significant similarity to SDRs from *Camellia sinensis* (61% identity), *Phaseolus lunatus* (61% identity), *Lactuca sativa* (57% identity), *A. annua* (56% identity), and *Z. zerumbet*

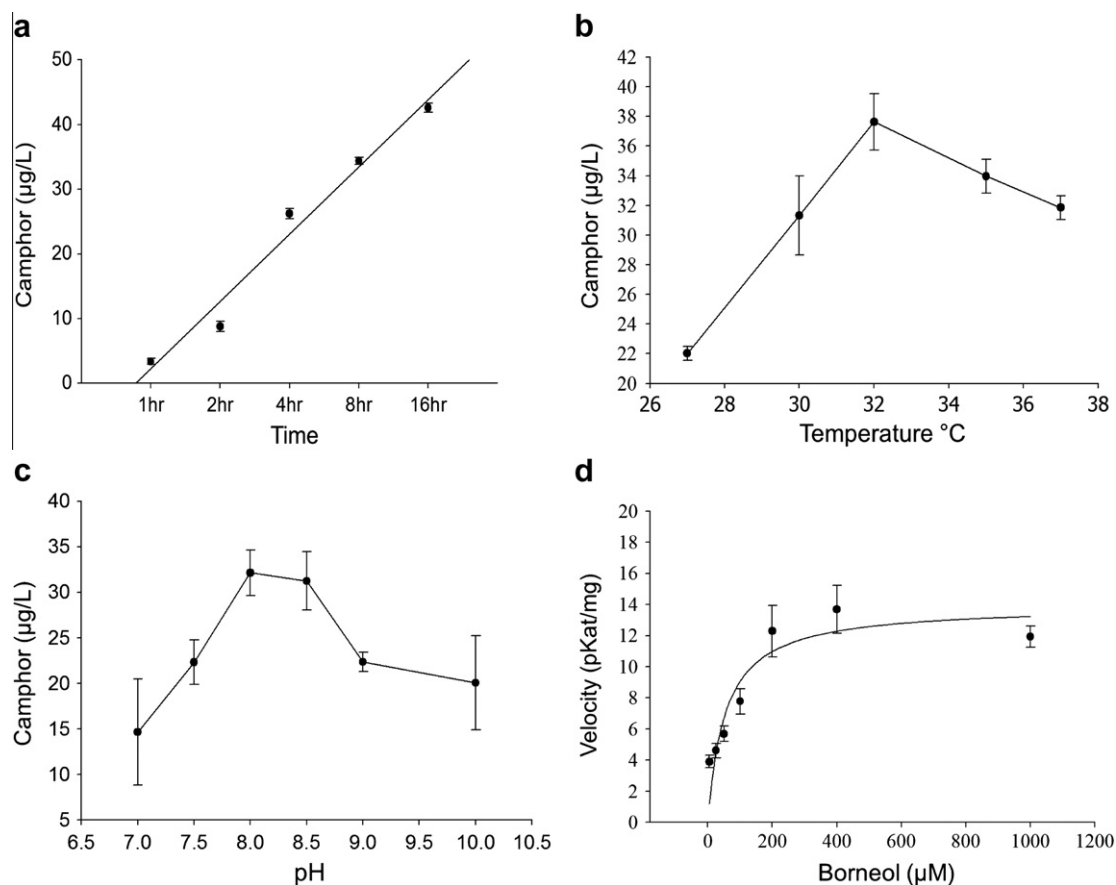


Fig. 3. Kinetic assay of LiBDH with borneol as a substrate: (a) time course assay of LiBDH activity, (b) effect of pH on LiBDH activity, (c) effect of temperature on LiBDH activity and (d) velocity of LiBDH at increasing borneol concentrations.

(52% identity) in multiple sequence alignment (Fig. 5), and was closely rooted with the above SDRs in the phylogenetic tree (Fig. 6).

Discussion

The secretory cells of glandular trichomes in *Lavandula* strongly and specifically express genes required for all stages of monoterpene metabolism, including those involved in the MEP pathway (e.g., DXS), which supplies precursor for monoterpene biosynthesis, and those that catalyze the formation of individual monoterpenes from GPP (e.g., linalool synthase; [4]). Also, genes encoding enzymes that catalyze the downstream modification of monoterpenes are strongly expressed in these trichomes. For example, the oxygenases, reductases and dehydrogenases that mediate the transformation of limonene to menthol in peppermint, a process that involves several biochemical reactions, are highly abundant in peppermint oil glands [27]. In order to probe the biosynthesis of EO monoterpene constituents in *Lavandula*, we have recently developed a gland-specific EST library from *L. x intermedia*. This database is highly enriched in monoterpene biosynthetic genes, and has facilitated the cloning of several terpene synthases including the *L. x intermedia* 1,8-cineole synthase [22]. We thus hypothesized that a borneol dehydrogenase is also strongly expressed in *L. x intermedia* oil glands, and proceeded to clone and functionally characterize the gene. Initially, we isolated two candidates from our *L. x intermedia* gland cDNA library, expressed them in *E. coli* cells, and assayed the dehydrogenase activities of the purified recombinant proteins using borneol and other main *Lavandula* monoterpenes as substrates. One of these candidates, LiBDH, was able to convert borneol into camphor. However, unlike many other

SDRs, including a recently reported *A. annua* SDR (ADH2; [16]) that accepts a number of substrates; LiBDH did not produce detectable products from other monoterpene alcohols, indicating that this SDR is highly specific. Indeed to our knowledge, LiBDH is the first borneol specific dehydrogenase reported from plants. The recently reported *A. annua* SDR (ADH2) was shown to dehydrogenate a range of substrates including: (–)-cis-carveol, (–)-artemisia alcohol, (+/–)-borneol, (–)-trans-carveol, and (–)-trans-pinocarveol. This enzyme had the highest specific activities for (–)-cis-carveol and (–)-artemisia alcohol, and the lowest specific activity for borneol [16], indicating that borneol is not a primary substrate for *A. annua* ADH2.

LiBDH is structurally similar to other plant SDRs and contains the standard conserved motifs present in these proteins, including the structural “Rossmann fold” and the “Ser-Tyr-Lys” catalytic triad which is very important for SDR functionality [28]. The protein also contains other conserved motifs present in plant SDRs including the N-terminal cofactor-binding motif TGxxx(AG)xG motif, and the catalytic YxxxK motif (Fig. 5) hence belongs to the classical SDR subfamily (Fig. 6). In addition, several key amino acid residues were conserved, including the Ser¹⁴¹ residue, which helps to form the catalytic triad “Ser-Tyr-Lys” [29], and the Asp⁴² residue that plays a critical role in determining the coenzyme (NAD⁺ over NADP⁺) specificity of SDRs [17,18,30,31].

The recombinant LiBDH had an optimum pH of 8.5, an optimum temperature of 32 °C, a K_m of 53.6 µM, a turnover number (k_{cat}) of $4.0 \times 10^{-4} \text{ s}^{-1}$, and a specificity constant (k_{cat}/K_m) of $7.5 \times 10^{-6} - \mu\text{M}^{-1} \text{ s}^{-1}$. Although most of these values are in the general range of those reported for other SDRs, we noted that LiBDH is a rather slow enzyme as long incubation times were required to obtain sufficient

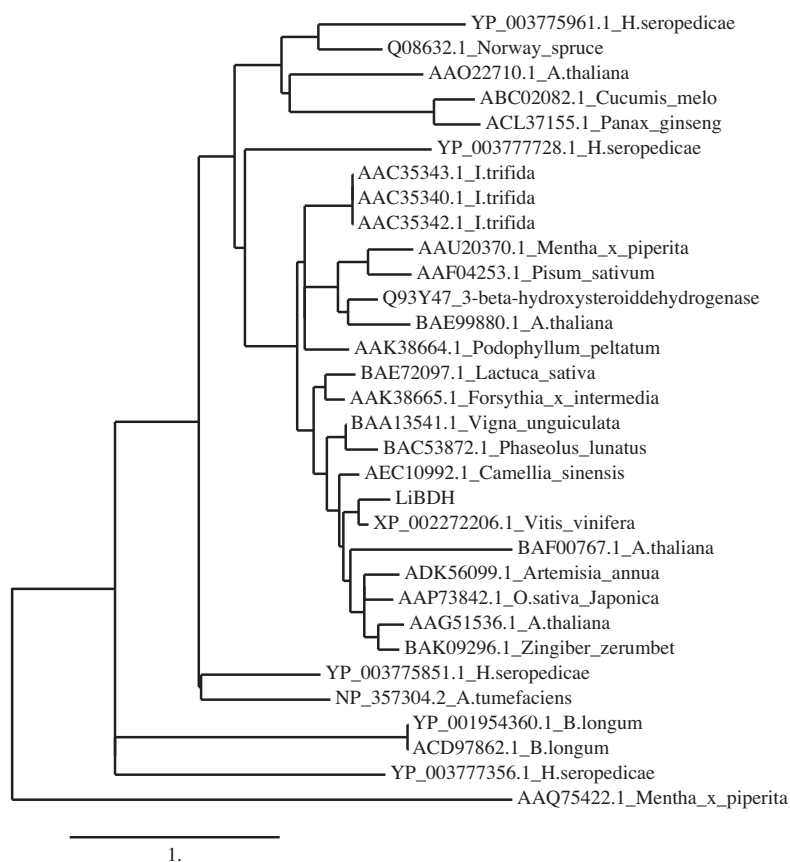


Fig. 6. Phylogenetic tree analysis of the “Classical Group” of plant SDRs. The scale bar represents 1.0 amino acid substitutions per site.

flower development (Fig. 4b). The tissue camphor content also remained unchanged, although the tissue concentration of borneol (the precursor to camphor) increases with flower age (Fig 4 d). The increases in the concentrations of the substrate implies a lack of its turnover, which in turn suggests that catalytically active LiBDH may be restricted to young tissue, where the bulk of camphor is produced, and not available during the latter stages of flower development. Consistent with these results, the activity of a number of monoterpenes synthases were very high during the early stages of leaf development (when EO synthesis is very active) and dropped rapidly in maturing leaves in peppermint [33]. Our data cannot explain whether the postulated “unavailability” of active LiBDH in older flowers is due to a lack of protein synthesis (i.e., inhibition of *LiBDH* mRNA translation), protein inactivation by inhibition, sub-cellular localization or another mechanism [34,35].

Like other plant terpene synthases [22,36], the *LiBDH* transcripts were highly concentrated in floral glandular trichomes of *L. x intermedia* (Fig. 4b). In this sense, the expression of *LiBDH* correlated with the expression of other genes involved in monoterpenoid metabolism in lavenders [22]. A surprising finding of this study was that *LiBDH* transcripts were present at higher levels in *L. angustifolia*, and *L. x intermedia* flowers, compared to those of *L. latifolia* plants (Fig. 4c). Given that *L. latifolia* plants produce camphor as a major EO constituent and are expected to express a borneol dehydrogenase gene strongly [37], our data imply that *L. latifolia* plants may express a unique BDH, and that *L. x intermedia* (which is a natural hybrid of *L. angustifolia* and *L. latifolia*) inherited its *LiBDH* from the *L. angustifolia* parent. This postulate is supported by the finding that both *L. angustifolia* and *L. x intermedia*-but not *L. latifolia* plants-express the *LiBDH*.

In conclusion, we have cloned a short chain alcohol dehydrogenase from *L. x intermedia* that converts borneol to camphor. Our

transcriptional activity data indicated that the gene is specifically expressed in glandular trichomes, and was likely inherited from *L. angustifolia*. Further, our data indicated that another *Lavandula* BDH may exist that is expressed in *L. latifolia* plants. To clone this gene the future efforts must concentrate on an EST database derived from oil glands of *L. latifolia* plants.

Acknowledgment

This work was supported through grants or in-kind contributions to Soheil Mahmoud by UBC Okanagan, Natural Sciences and Engineering Research Council of Canada, Investment Agriculture Foundation of British Columbia, and NRC Plant Biotechnology Institute through the NAPGEN program. We are grateful to Dr. Mark Rheault and Dr. Kirsten Wolthers of UBC Okanagan for their advice on the enzyme kinetic analysis. Finally, we thank Dr. Tim Upson of the University of Cambridge for the gift of *L. latifolia* tissue.

References

- [1] T. Upson, S. Andrews, G. Harriott, C. King, J. Langhorne, The Genus *Lavandula*, Timber Press, Portland, Oregon, 2004.
- [2] M. Lis-Balchin, Chemical composition of essential oils from different species, hybrids, and cultivars of *Lavandula*, in: M. Lis-Balchin (Ed.), *Lavender: The Genus Lavandula*, Taylor and Francis, London, 2002, pp. 251–262.
- [3] H.M.A. Cavanagh, J.N. Wilkinson, *Phytother. Res.* 16 (2002) 301–308.
- [4] A. Lane, A. Boeckleemann, G.N. Woronuk, L. Sarker, S.S. Mahmoud, *Planta* 231 (2010) 835–845.
- [5] J.G.W. Theis, G. Koren, *Can. Med. Assoc. J.* 152 (1995) 1821–1824.
- [6] H.X. Xu, N.T. Blair, D.E. Clapham, *J. Neurosci.* 25 (2005) 8924–8937.
- [7] D. Guilandcumming, G.J. Smith, *Experientia* 35 (1979) 659.
- [8] H.C. Goel, A.R. Roa, *Cancer Lett.* 43 (1988) 21–27.
- [9] C. Muller, *Curr. Contents/Agric. Biol. Environ. Sci.* (1982) 20.
- [10] S. Okamoto, F. Yu, H. Harada, T. Okajima, J. Hattan, N. Misawa, R. Utsumi, *FEBS J.* 278 (2011) 2892–2900.

- [11] G. Woronuk, Z. Demissie, M. Rheault, S. Mahmoud, *Planta Med.* 77 (2011) 7–15.
- [12] R. Croteau, F. Karp, *Biochem. Biophys. Res. Commun.* 72 (1976) 440–447.
- [13] R.B. Croteau, J.J. Shaskus, B. Renstrom, N.M. Felton, D.E. Cane, A. Saito, C. Chang, *Biochemistry (NY)* 24 (1985) 7077–7085.
- [14] F. Chen, D. Tholl, J. Bohlmann, E. Pichersky, *Plant J.* 66 (2011) 212–229.
- [15] P. Dewick, *Medicinal Natural Products: A Biosynthetic Approach*, Wiley & Sons Ltd., New York, NY, USA, 2004.
- [16] D.R. Polichuk, Y. Zhang, D.W. Reed, J.F. Schmidt, P.S. Covello, *Phytochemical* 71 (2010) 1264–1269.
- [17] K.L. Kavanagh, H. Jornvall, B. Persson, U. Oppermann, *Cell. Mol. Life Sci.* 65 (2008) 3895–3906.
- [18] Y. Kallberg, U. Oppermann, B. Persson, *FEBS J.* 277 (2010) 2375–2386.
- [19] M.G. Rossmann, A. Liljas, C.I. Brandén, L.J. Banaszak, *The Enzyme*, Academic Press, New York, 1975.
- [20] G. Labesse, A. Vidalcros, J. Chomilier, M. Gaudry, J.P. Mornon, *Biochem. J.* 304 (1994) 95–99.
- [21] N. Tanaka, T. Nonaka, K. Nakamura, A. Hara, *Curr. Org. Chem.* 5 (2001) 89–111.
- [22] Z.A. Demissie, M.A. Cella, L.S. Sarker, T.J. Thompson, M.R. Rheault, S.S. Mahmoud, *Plant Mol. Biol.* 79 (2012) 393–411.
- [23] R. Croteau, C.L. Hooper, M. Felton, *Arch. Biochem. Biophys.* 188 (1978) 182–193.
- [24] A. Ryden, C. Ruyter-Spira, R. Litjens, S. Takahashi, W. Quax, H. Osada, H. Bouwmeester, O. Kayser, *Plant Cell Physiol.* 51 (2010) 1219–1228.
- [25] L. Falk, K. Biswas, A. Boeckelmann, A. Lane, S.S. Mahmoud, *J. Essent. Oil Res.* 21 (2009) 225–228.
- [26] A. Dereeper, V. Guignon, G. Blanc, S. Audic, S. Buffet, F. Chevenet, J.F. Dufayard, S. Guindon, V. Lefort, M. Lescot, J.M. Claverie, O. Gascuel, *Nucleic Acids Res.* 36 (2008) W465–W469.
- [27] R. Croteau, E. Davis, K. Ringer, M. Wildung, *Naturwissenschaften* 92 (2005) 562–577.
- [28] Z. Chen, J. Jiang, Z. Lin, W. Lee, M. Baker, S. Chang, *Biochemistry (NY)* 32 (1993) 3342–3346.
- [29] O.A.B.S.M. Gani, O.A. Adekoya, L. Giurato, F. Spyarakis, P. Cozzini, S. Guccione, J. Winberg, I. Sylte, *Biophys. J.* 94 (2008) 1412–1427.
- [30] Y. Kallberg, U. Oppermann, H. Jornvall, B. Persson, *Protein Sci.* 11 (2002) 636–641.
- [31] K.L. Ringer, M.E. McConkey, E.M. Davis, G.W. Rushing, R. Croteau, *Arch. Biochem. Biophys.* 418 (2003) 80–92.
- [32] S. Mahmoud, R. Croteau, *Proc. Natl. Acad. Sci. USA* 100 (2003) 14481–14486.
- [33] M. McConkey, J. Gershenzon, R. Croteau, *Plant Physiol.* 122 (2000) 215–223.
- [34] D.K. Ro, J. Ehltling, C.J. Douglas, *Plant Physiol.* 130 (2002) 1837–1851.
- [35] G. Turner, R. Croteau, *Plant Physiol.* 136 (2004) 4215–4227.
- [36] Y. Iijima, D.R. Gang, E. Fridman, E. Lewinsohn, E. Pichersky, *Plant Physiol.* 134 (2004) 370–379.
- [37] J. Munoz-Bertomeu, I. Arrillaga, J. Segura, *Biochem. Syst. Ecol.* 35 (2007) 479–488.